STARS

Retrospective Theses and Dissertations

1978

A Simple Multicoupled Band-Pass Active Filter Design Employs Resistor Summing to Provide Multicoupling

Talal K. Chatila
University of Central Florida

Part of the Engineering Commons

Find similar works at: https://stars.library.ucf.edu/rtd

University of Central Florida Libraries http://library.ucf.edu

STARS Citation

Chatila, Talal K., "A Simple Multicoupled Band-Pass Active Filter Design Employs Resistor Summing to Provide Multicoupling" (1978). *Retrospective Theses and Dissertations*. 280.
https://stars.library.ucf.edu/rtd/280

Showcase of Text, Archives, Research & Scholarship

A SIMPLE MULTICOUPLED BAND-PASS
ACTIVE FILTER DESIGN EMPLOYS RESISTOR
SUMMING TO PROVIDE
MULTICOUPLING

BY

TALAL K. CHATILA
B.S.E., University of South Florida, 1975

RESEARCH REPORT

Submitted in partial fulfillment of the requirements
for the degree of Master of Science in Engineering in
the Graduate Studies Program of the College of Engineering
of Florida Technological University

Orlando, Florida
1978

A SIMPLE MULTICOUPLED BAND-PASS

ACTIVE FILTER DESIGN EMPLOYS RESISTOR

SUMMING TO PROVIDE

MULTICOUPLING

BY

TALAL K. CHATILA

ABSTRACT

The purpose of this paper is to present a new design
configuration for multicoupled band-pass filter based on
Mason's loop rule, together with the negative feedback
topology and to compare it with Leap Frog (LF) and Follow
the Leader Feedback (FLF) design examples.

Director of Research Report

ACKNOWLEDGMENTS

CONTENTS

INTRODUCTION

In recent years, RC-active filters have replaced the more conventional LC passive ones in many applications in which the use of active filters leads to a smaller and cheaper product. Their main drawback is the relatively high sensitivity to variations of both the active and the passive components. Thus, an extensive search has been conducted to reduce their sensitivities.

Some of the efforts have been directed toward coupled structures in which feedback is used to improve the sensitivity. Two of the leading efforts are the LF (Leap-Frog) and FLF (Follow the Leader Feedback).

The purpose of this paper is to present a new design configuration for multicoupled band-pass filter based on Mason's loop rule, together with the negative feedback topology and to compare it with LF and FLF design examples.

NEGATIVE FEEDBACK TOPOLOGY

The negative feedback topology is sketched in Figure 1. It is called so because the RC network associated with it provides a feedback path to the negative input terminal of the op amp. The transfer function of Figure 1 can be defined in terms of:

a) The Feedforward Transfer Function, T_{ff}

$$T_{ff} = \left. \frac{V_1}{V_2} \right|_{V_3 = 0} \tag{1}$$

b) The Feedback Transfer Function, T_{fb}

$$T_{fb} = \left. \frac{V_1}{V_3} \right|_{V_2 = 0} \tag{2}$$

From Figure 1, we have

$$V_0 = (V^+ - V^-) A(s) \tag{3}$$

where, V_0 is the output voltage of a real op amp.

By superposition

$$V^- = T_{ff} V_{in} + T_{fb} V_0 \tag{4}$$

Since $V^+ = 0$, we get

$$\frac{V_o}{V_{in}} = \frac{-T_{ff}}{T_{fb} + 1/A(s)} \qquad (5)$$

For an ideal op amp. $(A = \infty)$ equation 5 becomes:

$$\frac{V_o}{V_{in}} = \frac{-T_{ff}}{T_{fb}} \qquad (6)$$
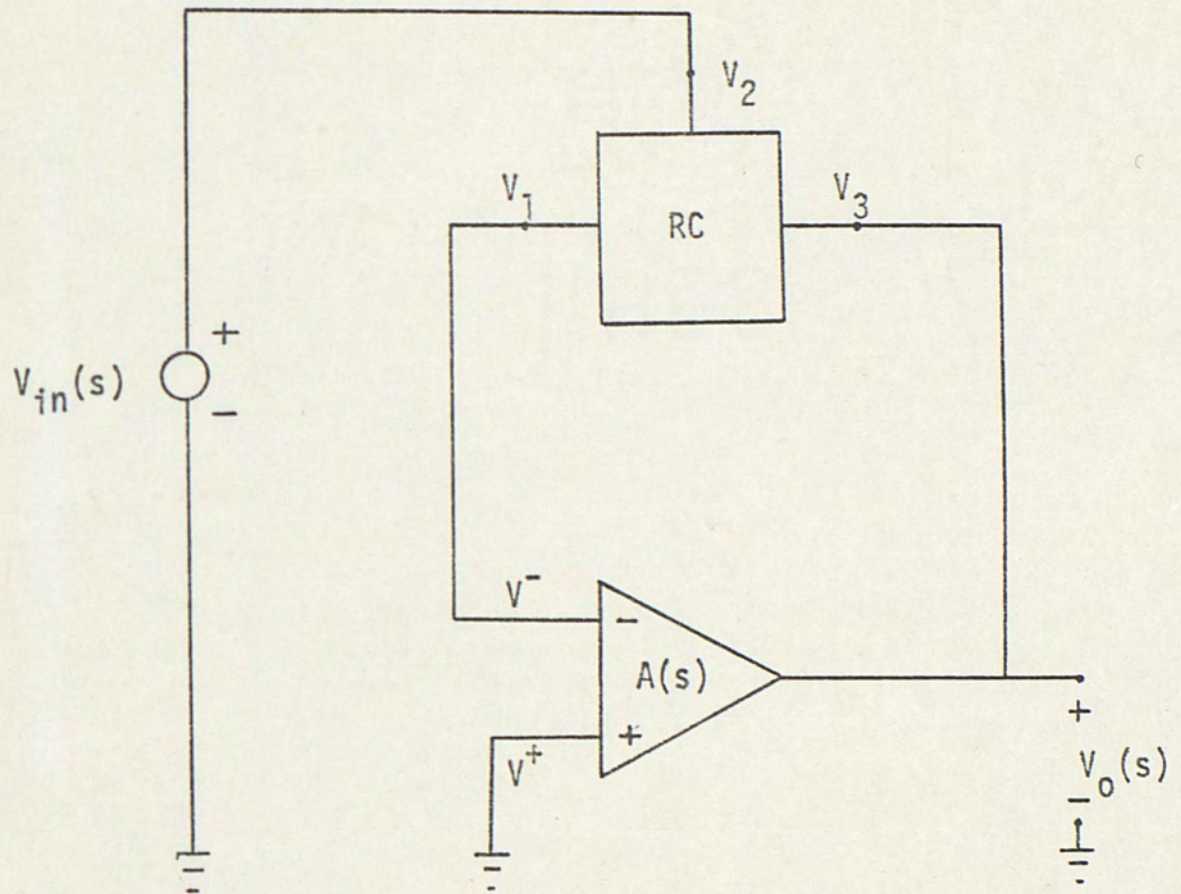
Figure 1.   The negative feedback topology.

A BAND-PASS CIRCUIT

A band-pass circuit based on the negative feedback topology will be developed. Consider the circuit shown in Figure 2, uses the bridged-T RC network of Figure 3. The nodal equations of this RC network are:

$$
\begin{bmatrix} sC_1 + sC_2 + 1/R_1 & -sC_1 \\ -sC_1 & sC_1 + 1/R_2 \end{bmatrix} \begin{bmatrix} V_x \\ V_1 \end{bmatrix} =
$$

$$
\begin{bmatrix} 1/R_1 & sC_2 \\ 0 & 1/R_2 \end{bmatrix} \begin{bmatrix} V_2 \\ V_3 \end{bmatrix} \tag{7}
$$

From equation (7) the feedback and feedforward transfer functions are found:

$$
T_{fb} = \left. \frac{V_1}{V_3} \right|_{V_2 = 0}
$$

$$
= \frac{s^2 + s(1/R_2C_1 + 1/R_2C_2) + 1/R_1R_2C_1C_2}{s^2 + s(1/R_2C_1 + 1/R_2C_2 + 1/R_1C_2) + 1/R_1R_2C_1C_2} \tag{8}
$$
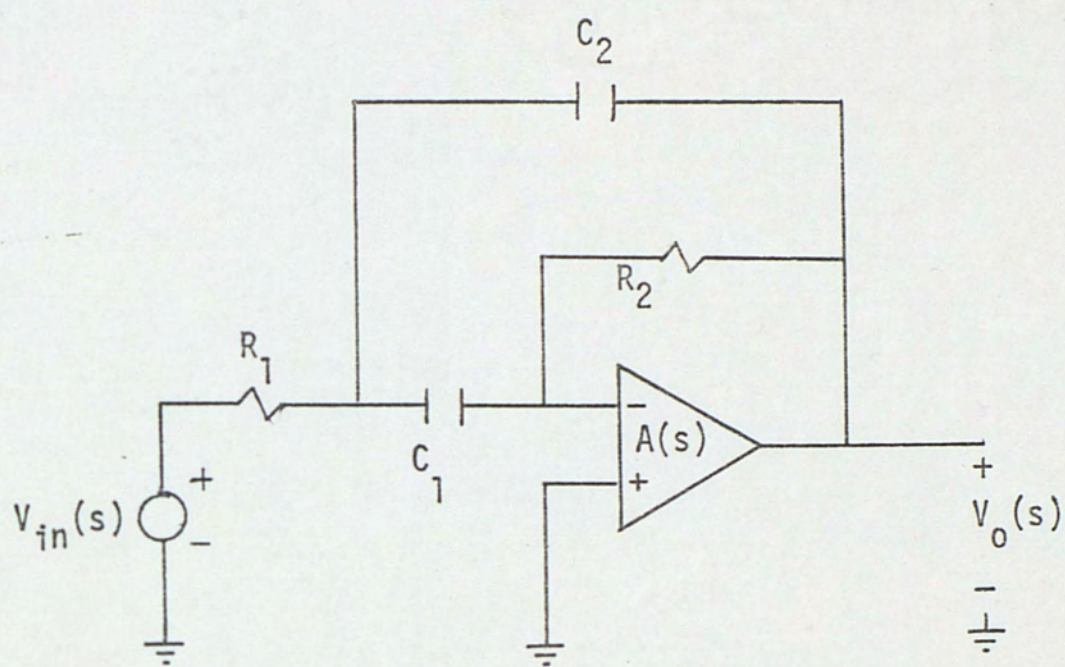
Figure 2. A band-pass circuit.
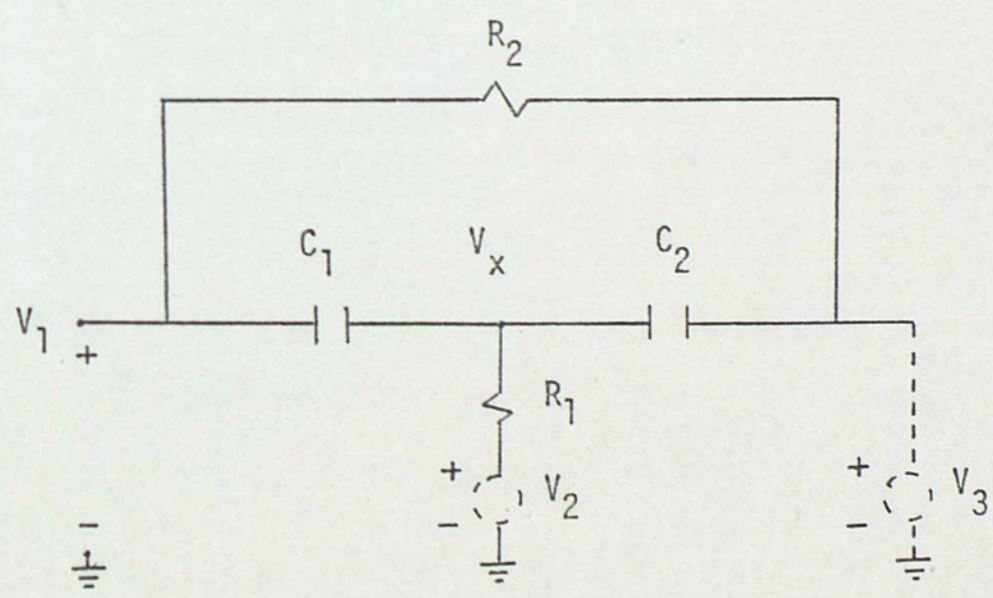
Figure 3. Bridge-T RC network.

And

$$T_{ff} = \left. \frac{V_1}{V_2} \right|_{V_3 = 0} \tag{9}$$

$$= \frac{s/R_1C_2}{s^2 + s(1/R_2C_1 + 1/R_2C_2 + 1/R_1C2) + 1/R_1R_2C_1C_2}$$

Using equation (6), assuming an ideal op amp, we get

$$\frac{V_o(s)}{V_{in}(s)} = \frac{-s/R_1C_2}{s^2 + s(1/R_2C_1 + 1/R_2C_2) + 1/R_1R_2C_1C_2} \tag{10}$$

$$= \frac{Ks}{s^2 + w_0s/Q_0 + w_0^2} \tag{11}$$

Where, w is defined to be omega

K is a constant

w_0 is the pole frequency

And Q_0 is a measure of the height and bandwidth at w_0

From equation (10) and equation (11) we have

$$w_0 = (1/R_1R_2C_1C_2)^{1/2} \tag{12}$$

$$Q_0 = \frac{(R_2/R_1)^{1/2}}{(C_2/C_1)^{1/2} + (C_1/C_2)^{1/2}} \qquad (13)$$

And

w_0, Q_0 and K are defined as the biquadratic parameters of equation (11).

The band-pass circuit developed in this section has low passive sensitivities, to show that this is so, let us synthesize equation (11) with equation (10).

From equation (12) and equation (13), and for $C_1 = C_2 = 1$ we get

$$R_1 = 1/2w_0Q_0 \qquad (14)$$

$$R_2 = 2Q_0/w_0 \qquad (15)$$

$$K = -1/R_1C_2 = -2w_0Q_0 \qquad (16)$$

To find the sensitivity of the biquadratic parameters of equation (11) to the elements, let us first consider the sensitivity of the pole frequency w_0 to change in a resistor R. Pole sensitivity is defined as the per-unit change in the pole frequency, $\Delta w_0/w_0$, caused by a per-unit change in the resistor, $\Delta R/R$

$$S_R^{w_0} = \lim_{\Delta R \to 0} \left[\frac{\Delta w_0/w_0}{\Delta R/R} \right] \qquad (17)$$

$$= \frac{R}{w_0} \frac{\partial w_0}{\partial R} \qquad (18)$$

$$S_R^{w_0} = \frac{\partial(\ln w_0)}{\partial(\ln R)} \qquad (19)$$

Likewise, the sensitivities of the parameter's w_0 and K to any element of the network are defined as:

$$S_C^{w_0} = \frac{C}{w_0} \frac{\partial w_0}{\partial C} \qquad (20)$$

$$S_R^K = \frac{R}{K} \frac{\partial K}{\partial R} \qquad (21)$$

etc.

In general, if a is a function of y, then

$$S_y^a = \frac{y}{a} \frac{\partial a}{\partial y} = \frac{\partial(\ln a)}{\partial(\ln y)} \qquad (22)$$

Using the equations developed above the component sensitivities for our example are:

$$S_{R_1}^{w_0} = S_{R_2}^{w_0} = S_{C_1}^{w_0} = S_{C_2}^{w_0} = -1/2 \qquad S_{R_1}^K = S_{C_2}^K = -1$$

$$S_{R_2}^{Q_0} = +1/2 \qquad S_{R_1}^{Q_0} = -1/2 \qquad S_{C_1}^{Q_0} = S_{C_2}^{Q_0} = 0$$

The magnitudes of the sensitivities are all less than one. A
sensitivity of one implies that a one percent change in a compon-
ent yields a one percent change in the parameter. This considered
a low sensitivity.

LOW-PASS TO BAND-PASS TRANSFORMATION

A very popular procedure for designing band-pass filters involves the use of a low-pass to band-pass geometric transformation. Using this approach, a low-pass prototype transfer function is first derived, and by means of the transformation is converted to a band-pass function.

In developing the transformation, the following notation will be employed:

p = low-pass prototype Laplace variable

s = band-pass final Laplace variable

w_0 = frequency scaling parameter in radians per second

Q_0 = quality factor

$G_{1p}(p)$ = low-pass prototype gain transfer function

$G_{bp}(s)$ = band-pass final gain transfer function

The low-pass to band-pass transformation is given by:

$$p = Q_0 \left(\frac{s^2 + w_0^2}{sw_0} \right) \qquad (23)$$

Practical utilization of the low-pass to band-pass transformation for determining a band-pass transfer function $G_{bp}(s)$ can be achieved as follows:

11

1)   Determine a low-pass transfer function $G_{lp}(p)$ in which the reference bandwidth B_{lp} is equal to the desired band-pass bandwidth B. This will usually require frequency scaling of the low-pass function if normalized design tables are used.

2)   Obtain the band-pass transfer function $G_{bp}(s)$, for a first order band-pass transfer function,

$$G_{bp}(s) \; = \; \frac{sw_0/Q_0}{s^2 + sw_0/Q_0 + w_0^2} \qquad\qquad (24)$$

$$= \; G_{lp}(p) \Bigg|_{p = Q_0 \; (\frac{s^2 + w_0^2}{sw_0})}$$

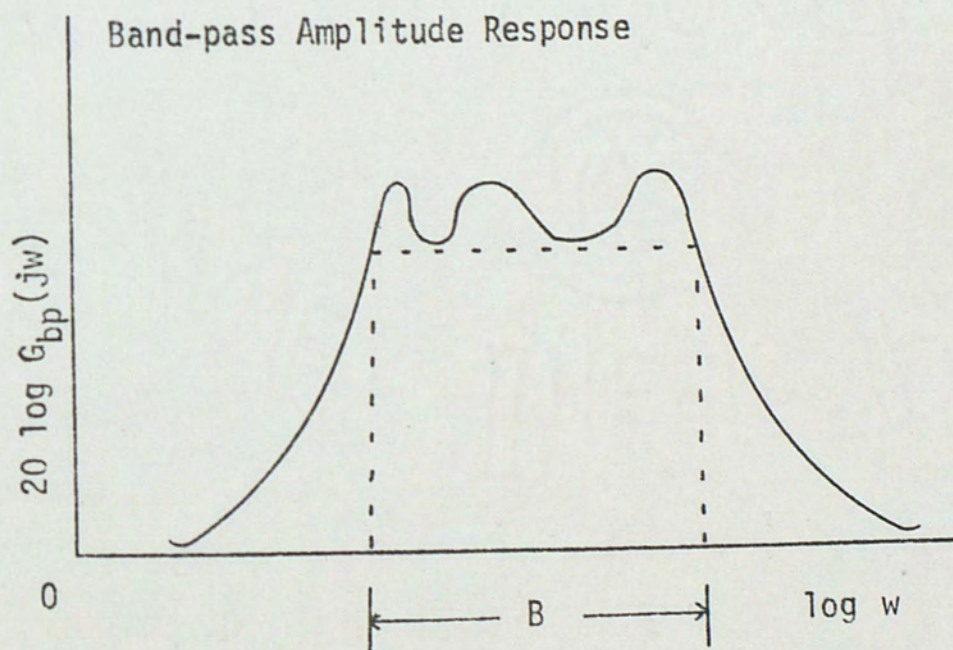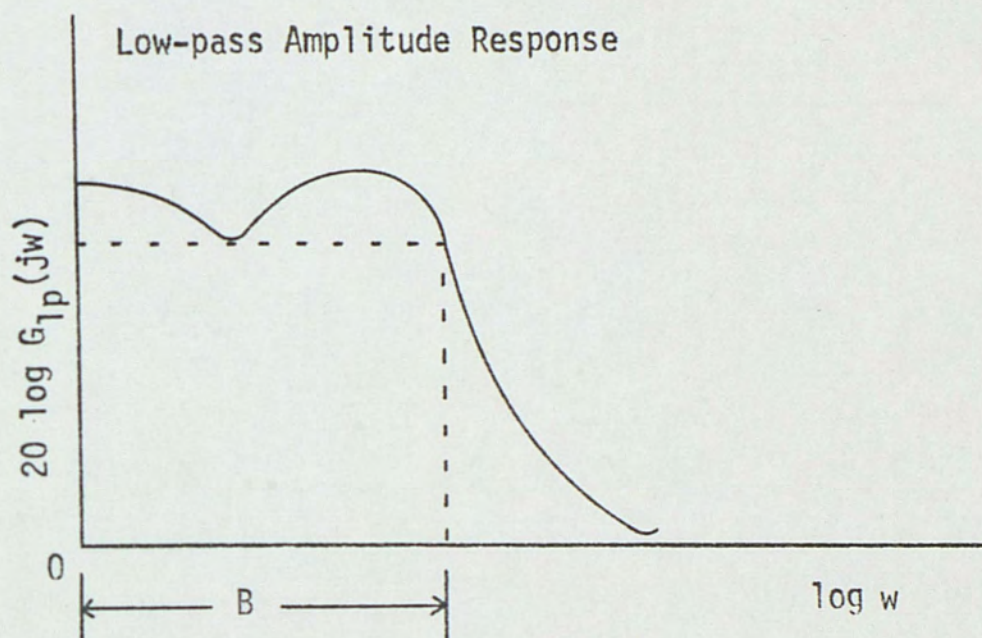$$= \; \frac{1}{p + 1} \qquad\qquad (25)$$

See Figure 4.

Figure 4.   Low-pass to band-pass transformation.

THE LF AND THE FLF REALIZATION

In this section the two established multicoupled band-pass feedback design techniques will be reviewed. The first of these techniques is the LF (Leap Frog) configuration. The second technique is the FLF (Follow the Leader Feedback) configuration. A second order Chebyshev low-pass normalized prototype with 1 dB ripple will be used as a design example to illustrate the LF and FLF techniques. In each design the band-pass circuit of Figure 2 will be used because of its simplicity and its low sensitivity.

LF Design Techniques:

The LF design techniques can be summarized by five steps:

1)   A passive ladder network that implements the normalized low-pass prototype transfer function is drawn.

2)   From the passive ladder network the branch-node equations are derived.

3)   A block diagram described by the branch-node equations of step 2 is drawn.

4)   Determine a low-pass to band-pass transformation on the elements of the block diagram of step 3.

5)   Using a band-pass configuration, the transformed elements of the block diagram of step 4 are implemented.

14

LF Design Example:

1) Consider the passive ladder network with normalized low-pass element values that will implement a second order Chebyshev low-pass prototype with 1 dB ripple, which is shown in Figure 5.
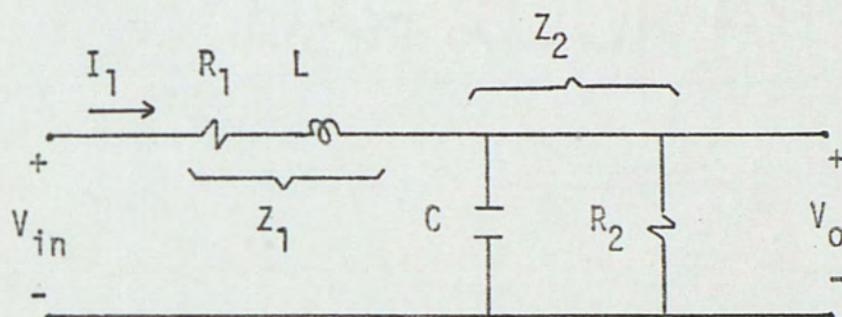

Figure 5.   A passive ladder network.

The transfer function is given by:

$$\frac{V_o(p)}{V_{in}(p)} = \frac{1}{1 + p(CR_p + L/R_s) + p^2 LCK} \tag{26}$$

Where

$$R_p = \frac{R_1 R_2}{R_1 + R_2} \qquad\qquad R_s = R_1 + R_2 \tag{27}$$

$$K = \frac{R_2}{R_1 + R_2}$$

$$\frac{V_o(p)}{V_{in}(p)} = \frac{1.10251}{p^2 + 1.09773p + 1.10251} \tag{28}$$

$$= \frac{1}{0.907021p^2 + 0.995664p + 1} \tag{29}$$

From equations (26), (27), and for $L = C = 1$ we get:

$$R_1 = 0.1030596$$

$$R_2 = 1.005358$$

2) The branch-node equations for Figure 5 are:

$$(V_{in}(p) - V_o(p)) \, 1/Z_1(p) = I_1(p) \tag{30}$$

Or

$$(V_{in}(p) - V_o(p)) \left(\frac{1}{0.1030596 + p} \right) = I_1(p) \tag{31}$$

And

$$V_o(p) = I_1(p) \, Z_2(p) \tag{32}$$

$$= I_1(p) \left(\frac{1}{0.9946706 + p} \right) \tag{33}$$

3) From the branch-node equations of step 2 a block diagram of the low-pass ladder normalized prototype was drawn. See Figure 6.
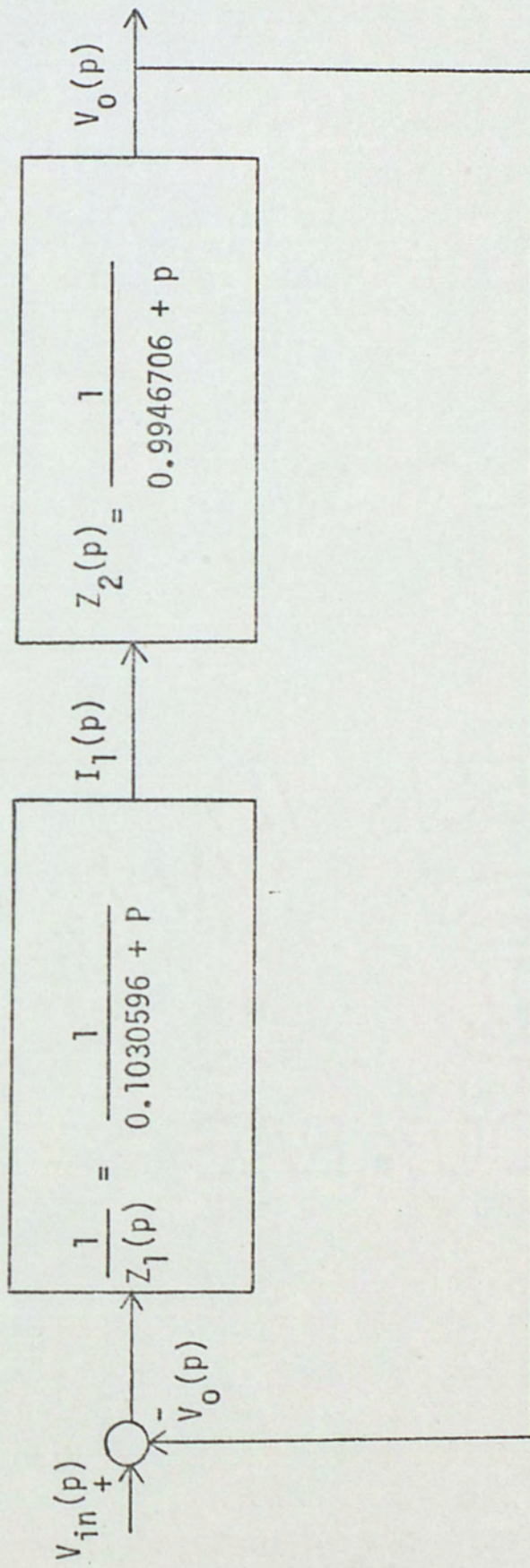
Figure 6.   A block diagram of the low-pass prototype.

4) Using the transformation described by equation (23), a
low-pass to band-pass transformation was performed to yield Figure
7.

$$\left. \frac{1}{Z_1(p)} \right|_{p = Q_0 \left(\frac{s^2 + w_0^2}{sw_0} \right)} = 1/Z_1(s) \tag{34}$$

$$= \frac{w_0 s/Q_0}{s^2 + 0.1030596 w_0 s/Q_0 + w_0^2} \tag{35}$$

And

$$\left. Z_2(p) \right|_{p = Q_0 \frac{(s^2 + w_0^2)}{sw_0}} = Z_2(s) \tag{36}$$

$$= \frac{w_0 s/Q_0}{s^2 + 0.9946706 w_0 s/Q_0 + w_0^2} \tag{37}$$

5) Using the band-pass configuration shown in Figure 2 and
implementing the transfer function for each transformed block in
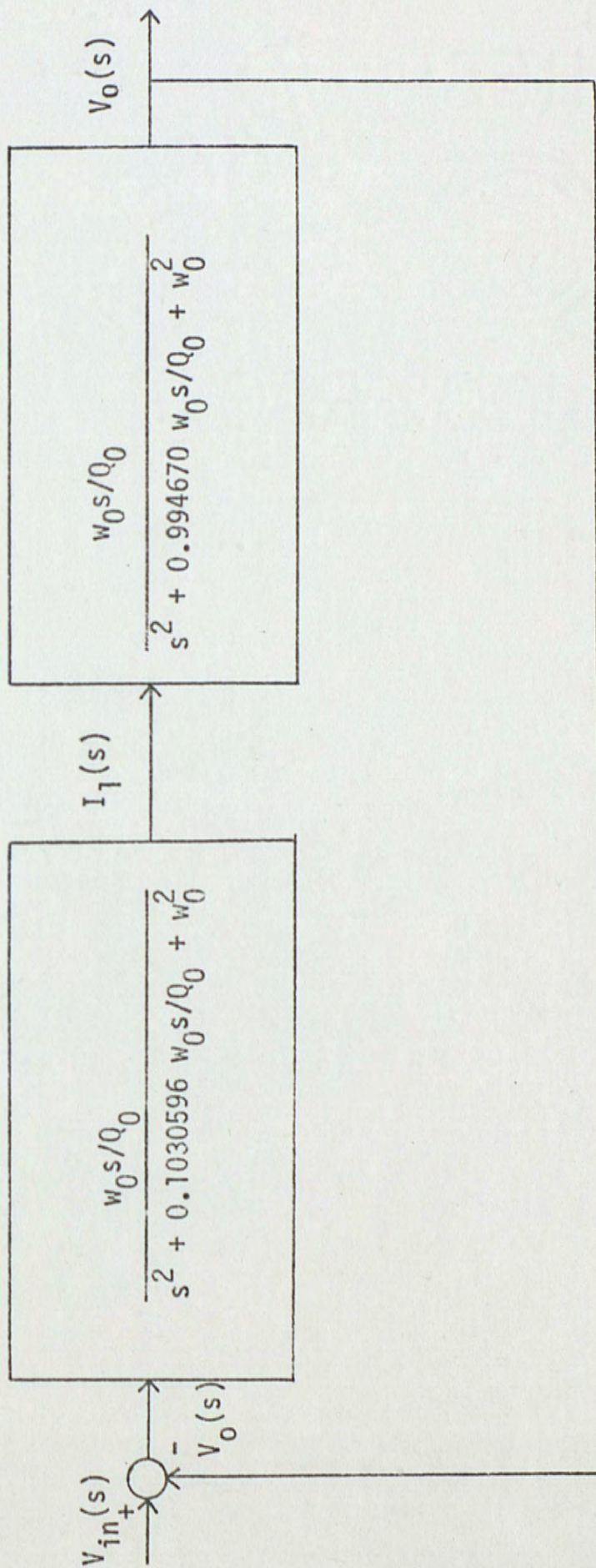the diagram shown in Figure 7 to get Figure 8.

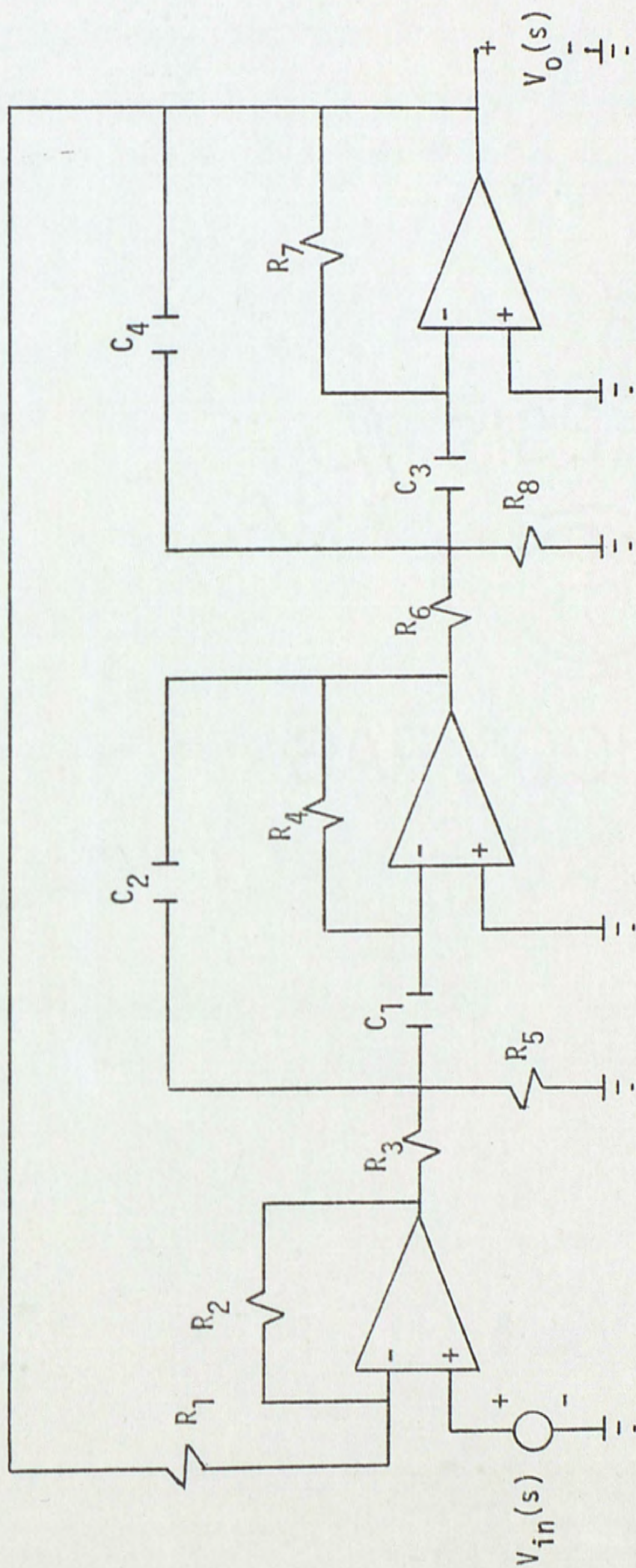Figure 7. A block diagram of the transformed prototype

Figure 8.   LF Circuit that implements the band-pass filter

FLF Design Techniques:

The FLF design techniques can be summarized by three steps:

1) The coefficients of the normalized low-pass prototype polynomial are determined, then the block diagram of the normalized low-pass prototype polynomial is drawn.

2) A low-pass to band-pass configuration is performed on each element of the block diagram.

3) Using a band-pass configuration capable of having Q = infinity, the transformed elements of the block diagram of step 2 are implemented.

FLF Design Example:

1) Given a second order Chebsyshev normalized low-pass pro-totype transfer function with 1 dB ripple.

$$G_2(p) = \frac{1.1025103}{p^2 + 1.09773p + 1.1025103} \tag{38}$$

The normalized low-pass prototype transfer function is given by:

$$G(p) = \frac{b_0}{\sum\limits_{k=0}^{n} a_k p^k} \tag{39}$$

Where

n = order

And

a_k = real coefficients

For

n = 2, G(p) becomes:

$$G(p) = \frac{b_0}{a_2 p^2 + a_1 p + a_0}$$ (40)

From equations (38) and (40) we get:

$b_0 = 1.1025103$

$a_2 = 1$

$a_1 = 1.0977343$ (41)

$a_0 = 1.1025103$

The coefficients above can be represented in a state variable model as it will be shown below:

Equation (39) is a special case of

$$T(p) = \frac{\sum\limits_{k=0}^{n-1} b_k p^k}{\sum\limits_{k=0}^{n} a_k p^k}$$ (42)

Where all $b_k = 0$ except b_0

For $a_0 = 1$ the above equation can be written as

$$T(p) = \sum_{k=0}^{n=1} \frac{b_k p^{k-n}}{1 - \sum_{k=0}^{n-1} -a_k p^{k-n}} \tag{43}$$

$$T(p) = \frac{\sum \text{forward paths}}{1 - \sum \text{feedback loops}} \tag{44}$$

which is a special case of Mason's loop rule. With the aid of
equation (43) the block diagram of the low-pass prototype is shown
in Figure 9. Notice that Figure 9 is the case where all the feed-
back loops sums at one node and the forward path is at the output
node. This configuration is called Follow the Leader Feedback.

2)   Using the transformation described by equation (23) a
low-pass to band-pass transformation was performed to yield Figure
10.

3)   Using the band-pass configuration shown in Figure 2 and
implementing the transfer function for each transformed block in the
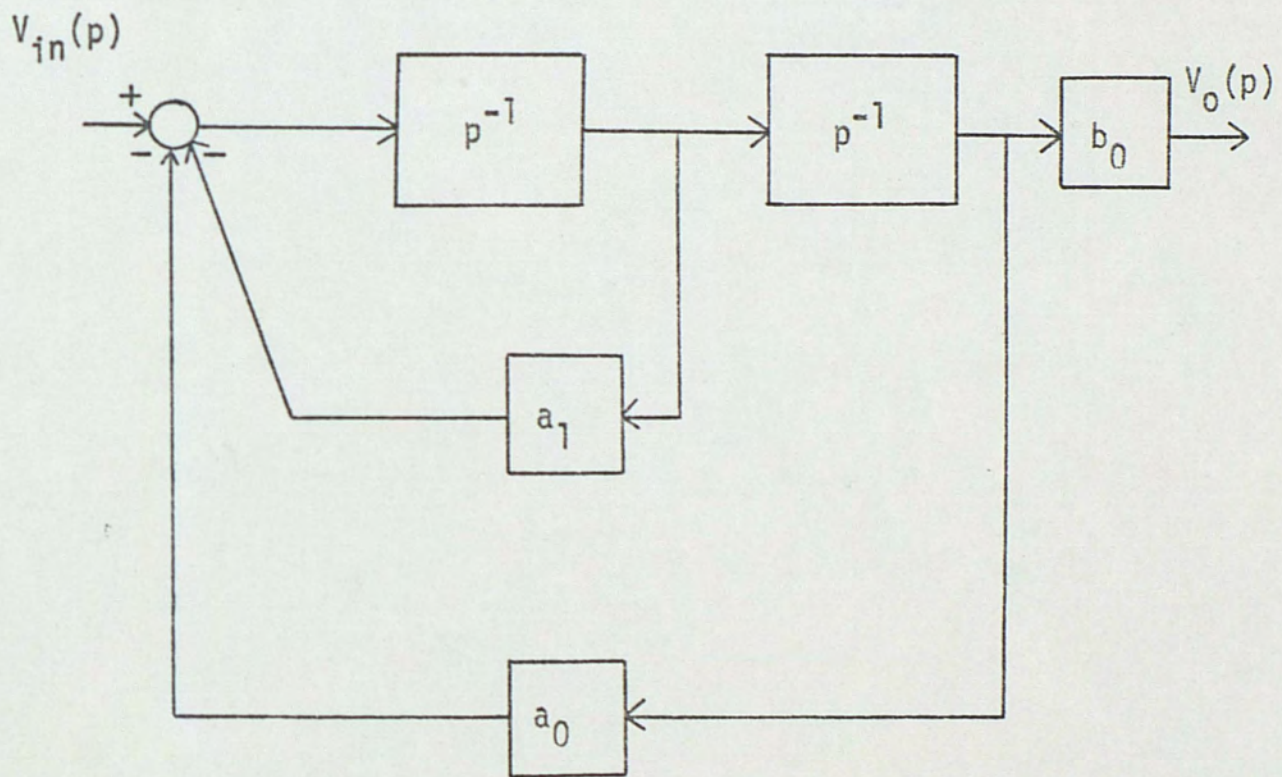diagram shown in Figure 10 to get Figure 11.

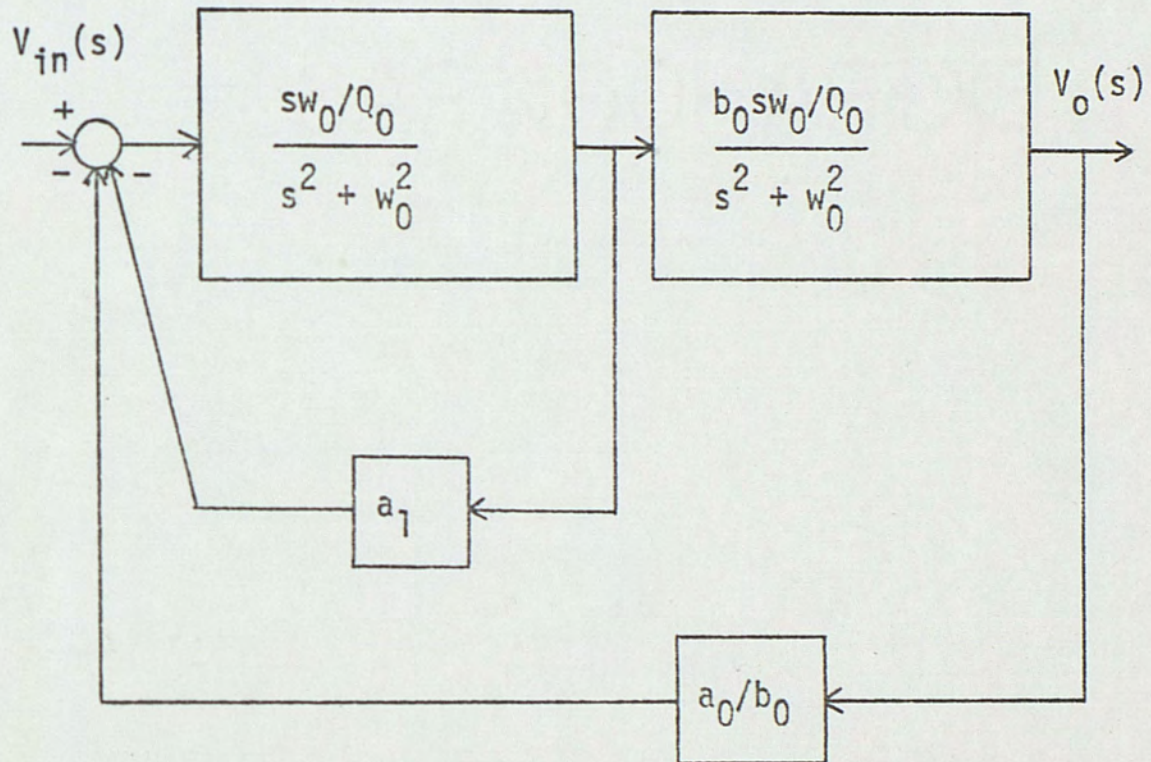Figure 9.   A Follow the Leader Feedback block diagram.

Figure 10.

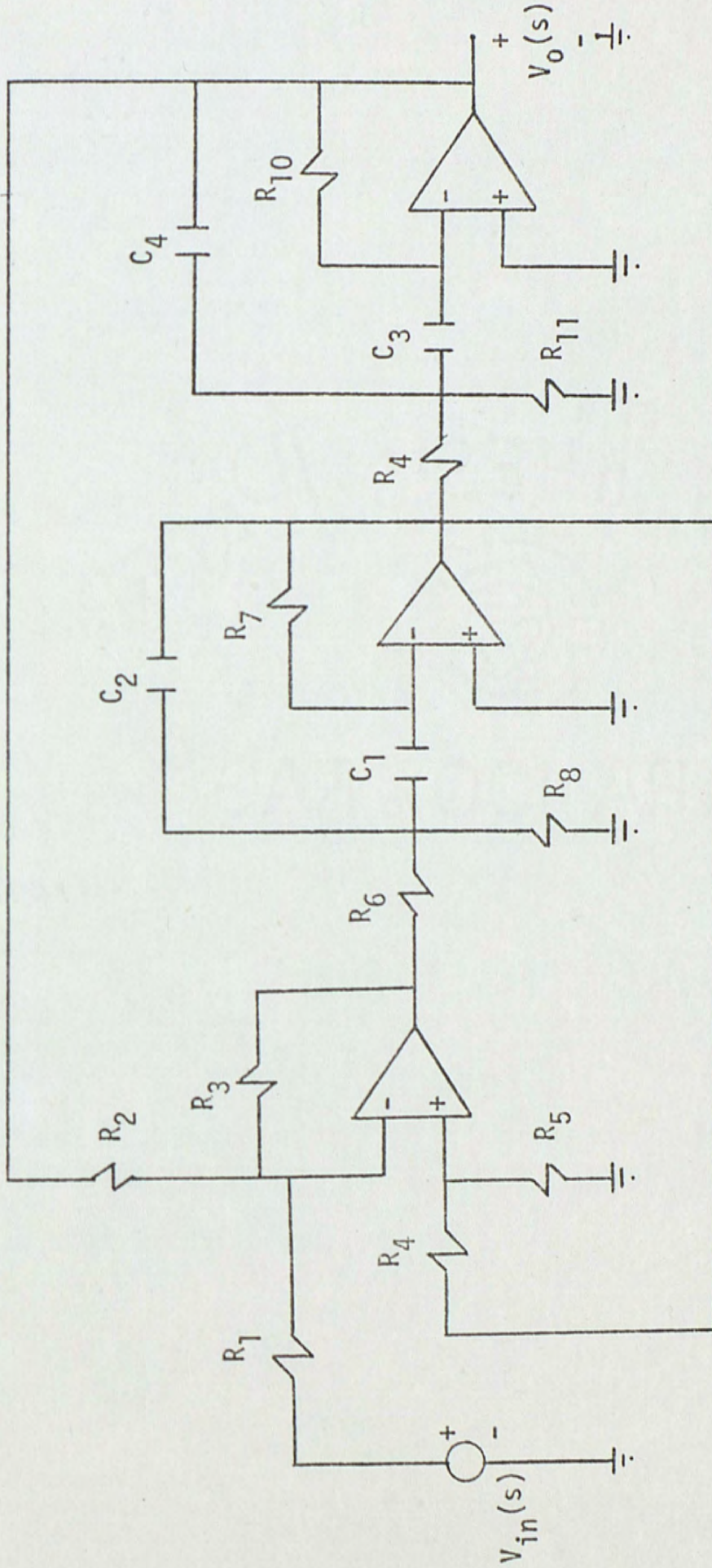A second order Follow the Leader Feedback band-pass filter

Figure 11. FLF circuit that implements the band-pass filter.

THE NEW DESIGN APPROACH
A SIMPLE MULTICOUPLED BAND-PASS FILTER

In the previous sections the negative feedback topology
was discussed, and a band-pass circuit based on the negative
feedback topology was developed. This band-pass circuit was
used in the LF and FLF examples because of its simplicity and
its low sensitivity.

In this section a new design approach based on equation (43)
will be developed. If two circuits as shown in Figure 2 are to be
operated as a feedback gain in a multicoupled mode, then a feed-
back path must be found. Implementing equation (43) is the circuit
of Figure 12. It will be shown that the circuit of Figure 12 can
be represented by a second order low-pass polynomial in the proto-
type domain.

Consider the transfer function between the various observable
test points. These transfer functions are:

1) $T_1(s) = \dfrac{V_o(s)}{V_{o1}(s)}$ (45)

$$T_2(s) = \dfrac{V_{o1}(s)}{V_{in}(s)} \Bigg|_{V_o = 0}$$ (46)
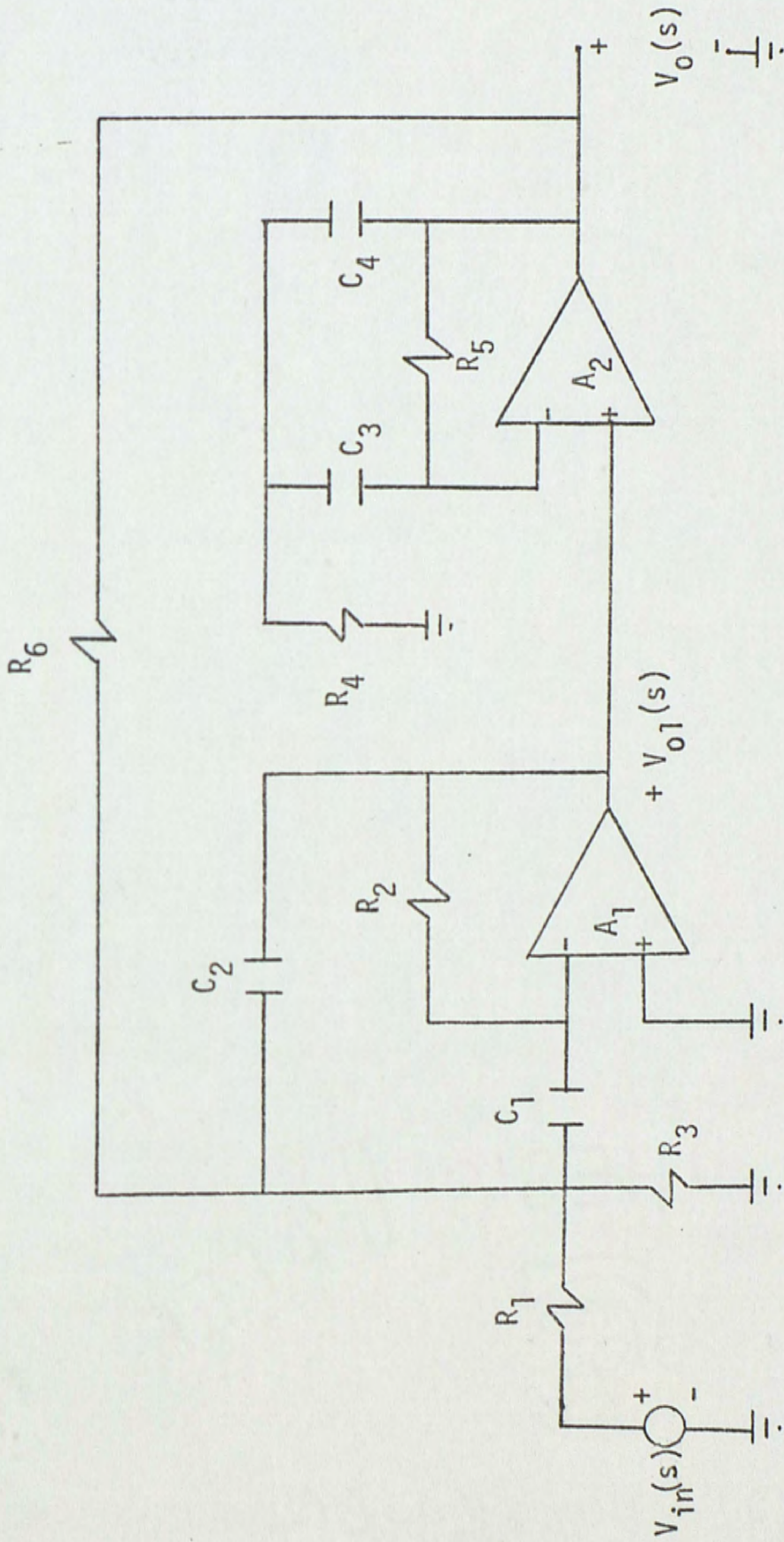
Figure 12. A second order band pass filter of the design to be implemented.

$$T_3(s) = \left. \frac{V_{o1}(s)}{V_o(s)} \right|_{V_{in} = 0} \tag{47}$$

$T_1(s)$ is found by analyzing Figure 13.
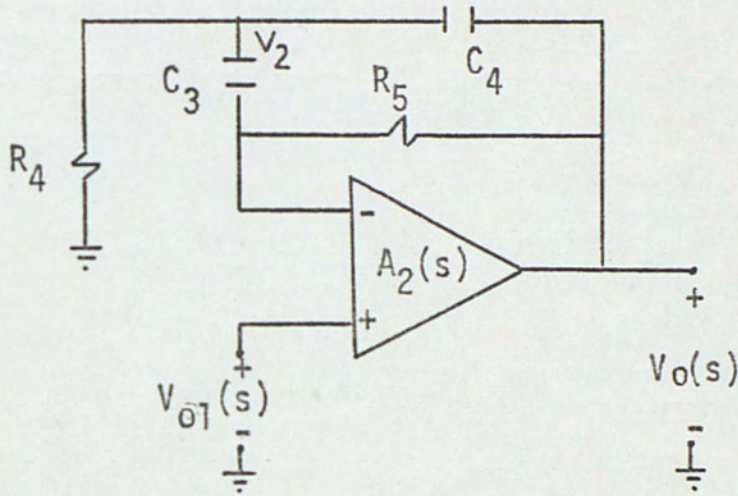
Figure 13.   Second stage of Figure 12.

For an ideal op amp, ($A_2 = \infty$) the nodal equations for Figure 13 are:

$$V_{o1} (1/R_5 + sC_3) - V_2 (sC_3) - V_o (1/R_5) = 0 \tag{48}$$

And

$$V_2 (1/R_4 + sC_3 + sC_4) - V_{o1}(sC_3) - V_o (sC_4) = 0 \tag{49}$$

Solving for V_2 in equation (48) yields

$$V_2 = V_{o1} (1/R_5 \, sC_3 + 1) - V_o (1/R_5 \, sC_3) \tag{50}$$

Substituting equation (50) into equation (49) yields

$$\frac{V_o(s)}{V_{o1}(s)} = \frac{s^2 C_4 R_4 R_5 C_3 + s(R_5 C_3 + R_4 (C_3 + C_4)) + 1}{s^2 C_4 R_4 R_5 C_3 + sR_4(C_3 + C_4) + 1} \qquad (51)$$

Similarly

$$T_2(s) = \left. \frac{V_{o1}(s)}{V_{in}(s)} \right|_{V_o = 0}$$

For an ideal op amp. $(A = \infty)$ the nodal equations of Figure 14 are:
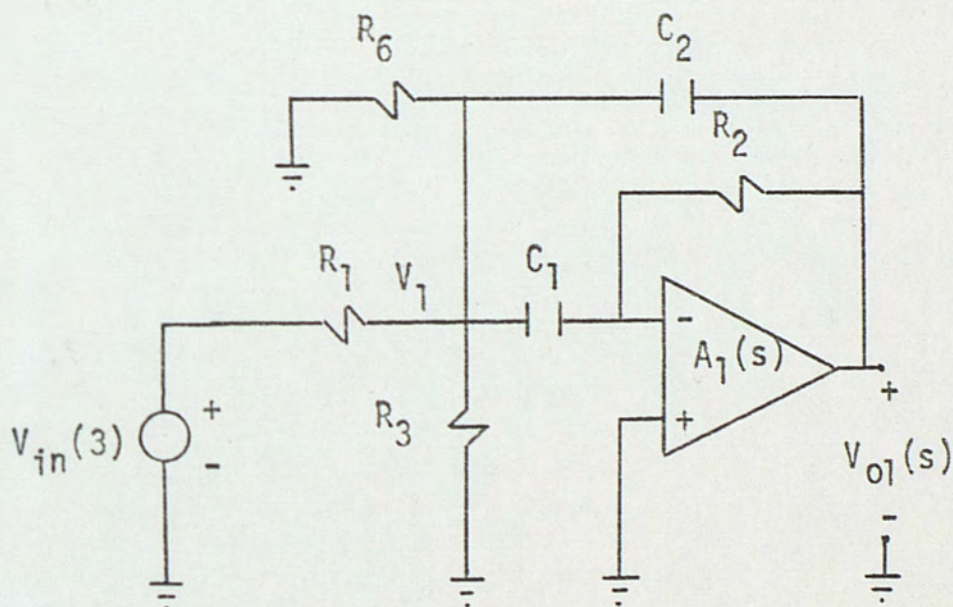
Figure 14. The stage of Figure 12 with the output grounded

$$V_1(sC_1 + 1/R_1 + 1/R_3 + 1/R_6 + sC_2) - V_{in}(1/R_1) - V_{o1} sC_2 = 0$$

$$(52)$$

$$-V_1 sC_1 - V_{o1} 1/R_2 = 0 \qquad (53)$$

Solving equations (52) and (53) to get:

$$\frac{V_{o1}(s)}{V_{in}(s)} = \frac{-R_2 s C_1 R_3 R_6 / (R_1 R_3 + R_1 R_6 + R_3 R_6)}{\dfrac{s^2 R_1 R_3 R_6 R_2 C_1 C_2}{R_1 R_3 + R_1 R_6 + R_3 R_6} + \dfrac{R_1 R_3 R_6 (C_1 + C_2) s}{R_1 R_3 + R_1 R_6 + R_3 R_6} + 1} \tag{54}$$

Similarly

$$T_3(s) = \left. \frac{V_{o1}(s)}{V_o(s)} \right|_{V_{in} = 0}$$
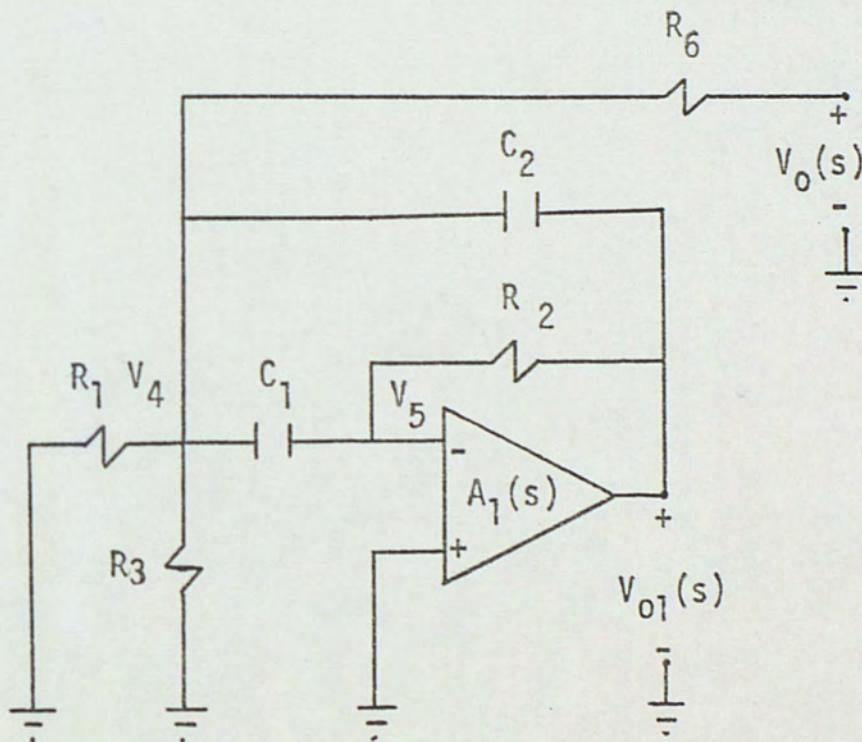
Figure 15.   The first stage of Figure 12

with the input grounded.

Again, the nodal equations of Figure 15, assuming an ideal op amp, $(A = \infty)$ are:

$$V_4(1/R_1 + 1/R_3 + 1/R_6 + s(C_1 + C_2)) - V_{o1}sC_2 - V_o1/R_6 = 0 \qquad (55)$$

$$-V_5sC_1 - V_{o1}1/R_2 = 0 \qquad (56)$$

Solving equations (55) and (56) to get:

$$\frac{V_{o1}(s)}{V_{in}(s)} = \frac{-R_2C_1sR_1R_3/(R_1R_3 + R_1R_6 + R_3R_6)}{\dfrac{s^2R_1R_3R_6R_2C_1C_2}{R_1R_3 + R_1R_6 + R_3R_6} + \dfrac{R_1R_3R_6(C_1 + C_2)\,s}{R_1R_3 + R_1R_6 + R_3R_6} + 1} \qquad (57)$$

Putting equations (51), (54) and (57) in the general form to get:

$$\frac{V_o(s)}{V_{o1}(s)} = \frac{s^2/w_1^2 + (1/w_1Q_1 + T)s + 1}{s^2/w_1^2 + s/w_1Q_1 + 1} \qquad (58)$$

Where $T = R_5C_3$

$$\qquad (59)$$

$$\qquad = 2Q_1/w_1 (\text{from equation 15})$$

$$\left.\frac{V_{o1}(s)}{V_{in}(s)}\right|_{V_o = 0} = \frac{-K_0s/w_2Q_2}{s^2/w_2^2 + s/w_2Q_2 + 1} \qquad (60)$$

And

$$\frac{V_{o1}(s)}{V_o(s)}\Bigg|_{V_{in} = 0} = \frac{-K_1 s/w_2 Q_2}{s^2/w_2^2 + s/w_2 Q_2 + 1} \tag{61}$$

In general, one can conveniently make $w_1 = w_2 = w_0$

and $Q_1 = Q_2 = Q_0$, then equations (58), (60) and (61) become:

$$\frac{V_o(s)}{V_{o1}(s)} = \frac{s^2/w_0^2 + (1/w_0 Q_0 + 2Q_0^2)\, s + 1}{s^2/w_0^2 + s/w_0 Q_0 + 1} \tag{62}$$

$$\frac{V_{o1}(s)}{V_{in}(s)}\Bigg|_{V_o = 0} = \frac{-K_0 s/w_0 Q_0}{s^2/w_0^2 + s/w_0 Q_0 + 1} \tag{63}$$

$$\frac{V_{o1}(s)}{V_o(s)}\Bigg|_{V_{in} = 0} = \frac{-K_1 s/w_0 Q_0}{s^2/w_0^2 + s/w_0 Q_0 + 1} \tag{64}$$

Now perform a band-pass to low-pass transformation using
equation (23) in equations (62), (63) and (64) yield:

$$\frac{V_o(s)}{V_{o1}(s)}\Bigg|_{p = \dfrac{Q(s^2 + w_0^2)}{sw_0}} = \frac{pQ_0/Q + 1\; 2Q_0^2}{pQ_0/Q + 1} \tag{65}$$

$$\left.\frac{V_{o1}(s)}{V_{in}(s)}\right| = \frac{-K_0}{pQ_0/Q + 1} \tag{66}$$

$$\left.\phantom{\frac{V_{o1}(s)}{V_{in}(s)}}\right|_{p} = \frac{Q(s^2 + w_0^2)}{sw_0}$$

$$\left.\frac{V_{o1}(s)}{V_o(s)}\right| = \frac{-K_1}{pQ_0/Q + 1} \tag{67}$$

$$\left.\phantom{\frac{V_{o1}(s)}{V_o(s)}}\right|_{p} = \frac{Q(s^2 + w_0^2)}{sw_0}$$

Where

$$Q = f_0/B$$

$$f_0 = \text{center frequency} \tag{68}$$

$$B = \text{bandwidth}$$

From equations (66), (67) and (68) the block diagram of Figure 12 is shown in Figure 16, and $V_o(p)/V_{in}(p)$ is given by equation (69).

$$\frac{V_o(p)}{V_{in}(p)} = \frac{-K_0(pQ_0/Q + 1 + 2Q_0^2)}{p^2Q_0^2/Q^2 + p(2 + K_1)Q_0/Q + K_1(1 + 2Q_0^2) + 1} \tag{69}$$
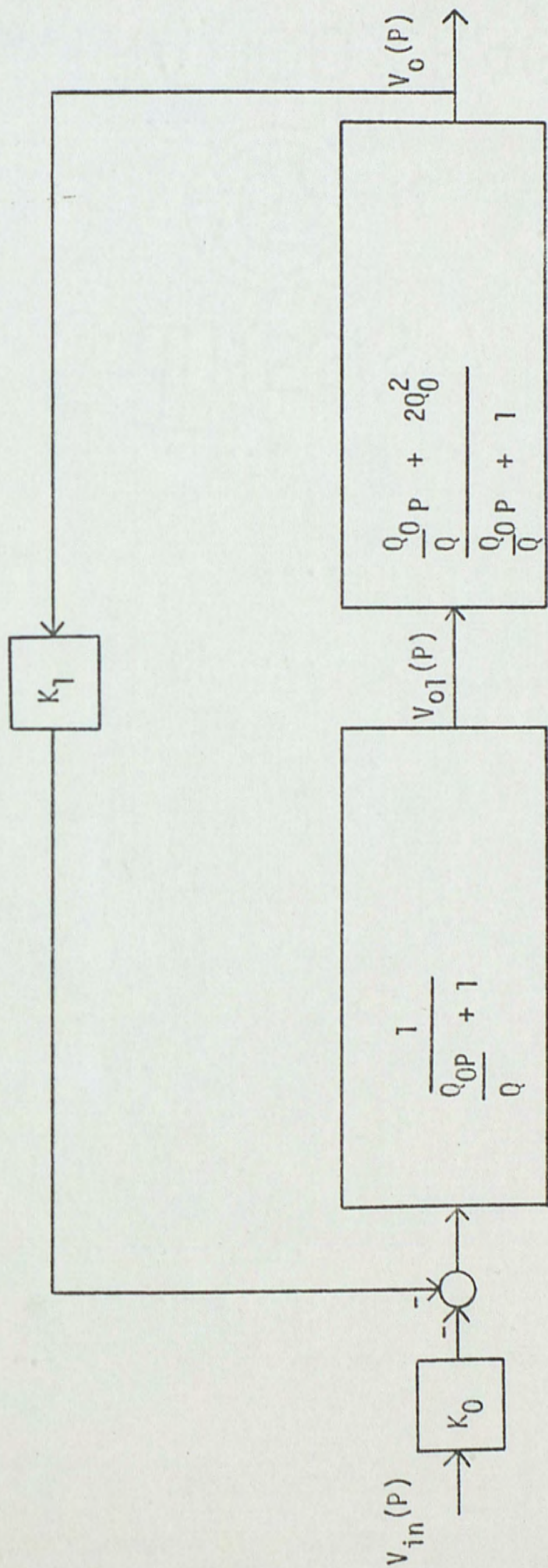
Figure 16. The block diagram of the low-pass prototype of the transformed band-pass filter

Divide equation (69) by $(Q_0/Q)^2$ yields

$$\frac{V_o(p)}{V_{in}(p)} = \frac{-K_0(p + 1 + 2Q_0^2) \, Q/Q_0) \, Q/Q_0}{p^2 + Q/Q_0(2 + K_1) \, p + (K_1 \, (1 + 2Q_0^2) + 1) \, (Q/Q_0)^2}$$

For $(1 + 2Q_0^2) \, Q/Q_0 >> 1$ and $K_1 << 2$ \hfill (71)

$V_o(p)/V_{in}(p)$ becomes

$$\frac{V_o(p)}{V_{in}(p)} = \frac{-K_0(1 + 2Q_0^2) \, (Q/Q_0)^2}{p^2 + 2pQ/Q_0 + (K_1 \, (1 + 2Q_0^2) + 1) \, (Q/Q_0)^2} \hfill (72)$$

In general form equation (72) may be written:

$$\frac{V_o(p)}{V_{in}(p)} = \frac{K}{p^2 + \alpha \Omega_0 p + \Omega_0^2} \hfill (73)$$

Where

$$\Omega_0 = (K_1 + 2K_1 \, Q_0^2 + 1)^{1/2} \, Q/Q_0 \hfill (74)$$

$$K = \frac{-K_0(1 + 2Q_0^2)}{K_1(1 + 2Q_0^2) + 1} \hfill (75)$$

$$\alpha = \frac{2}{(K_1 + 2K_1 Q_0^2 + 1)^{1/2}} \hfill (76)$$

Higher order cases based on equation (44) can be designed; but as the order goes up the open loop quality factor becomes too high and other methods must be used.

DESIGN EXAMPLE

Design a multicoupled band-pass filter based on the new design approach, having the following characteristics: a) The low-pass normalized Butterworth gain function given by:

$$G_{1p}(p) = \frac{10}{p^2 + 1.4142p + 1} \tag{77}$$

a)   The 3 dB bandwidth of 424 Hz

b)   The center frequency of 3000 Hz

Design Method:

Using equation (72) and equation (77) the open loop quality factor Q_0 is found:

$$2Q/Q_0 = 1.4142$$

or

$$Q_0 = Q1.4142$$

But Q is defined as:

$$Q = f_0/B$$

Therefore

$$Q_0 = 1.4142f_0/B$$

Also using equation (72) and (77) the feedback gain is found:

$$(\beta 2Q_0^2(1 + 2Q_0^2) + 1)(Q/Q_0)^2 = 1$$

or

$$\beta = 1/4Q_0^4 = R_3/R_6$$

where

$$K_1 = 2Q_0^2$$

From equations (54), (57) and (72) K_0 is found to be:

$$K_0 = R_6/2R_1$$

Select $C_1 = C_2 = C_3 = C_4 = C$

Therefore R_3 and R_4 are computed from equation (14)

$$R_3 = R_4 = 1/2Q_0 w_0 C$$

R_2 and R_5 are computed from equation (15)

$$R_2 = R_5 = 2Q_0/w_0 C$$

Design Example

A multicoupled band-pass Butterworth filter was designed to meet the requirements stated previously. Using the above information we have:

$$C_1 = C_2 = C_3 = C_4 = 0.0056 \,\mu F$$

$$R_3 = R_4 = 473 \,\Omega$$

$$R_2 = R_5 = 193 \,K\Omega$$

$$Q = f_0/B = 7.08$$

$$Q_0 = 10.01$$

$$R_6 = 19 \ M\Omega$$

$$R_1 = 1.90 \ M\Omega$$

The model circuit for the design example is shown in Figure 18. In manufacturing the circuit, all resistors and capacitors have manufacturing tolerance of ± 1 percent except R_1 and R_6; they have manufacturing tolerances of ± 5 percent. A Tee equivalent for R_6 is used for tolerance purpose, the Tee equivalent for R_6 is shown in Figure 17 and it is calculated as follows:

$$R_6 = \frac{R_a R_b + R_a R_c + R_b R_c}{R_c}$$

let $R_a = R_b = 1.9 \ M\Omega$

$$R_6 = 19 \ M = 1.9 + 1.9 + \frac{(1.9)^2}{R_c}$$

Solve to get $R_c = 237 \ K\Omega$

$$R_a = 1.9 \ M\Omega \quad R_b = 1.9 \ M\Omega$$
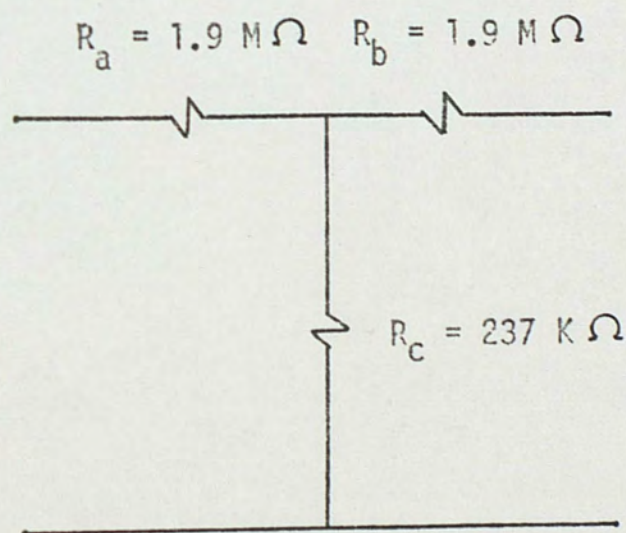
$$R_c = 237 \ K\Omega$$

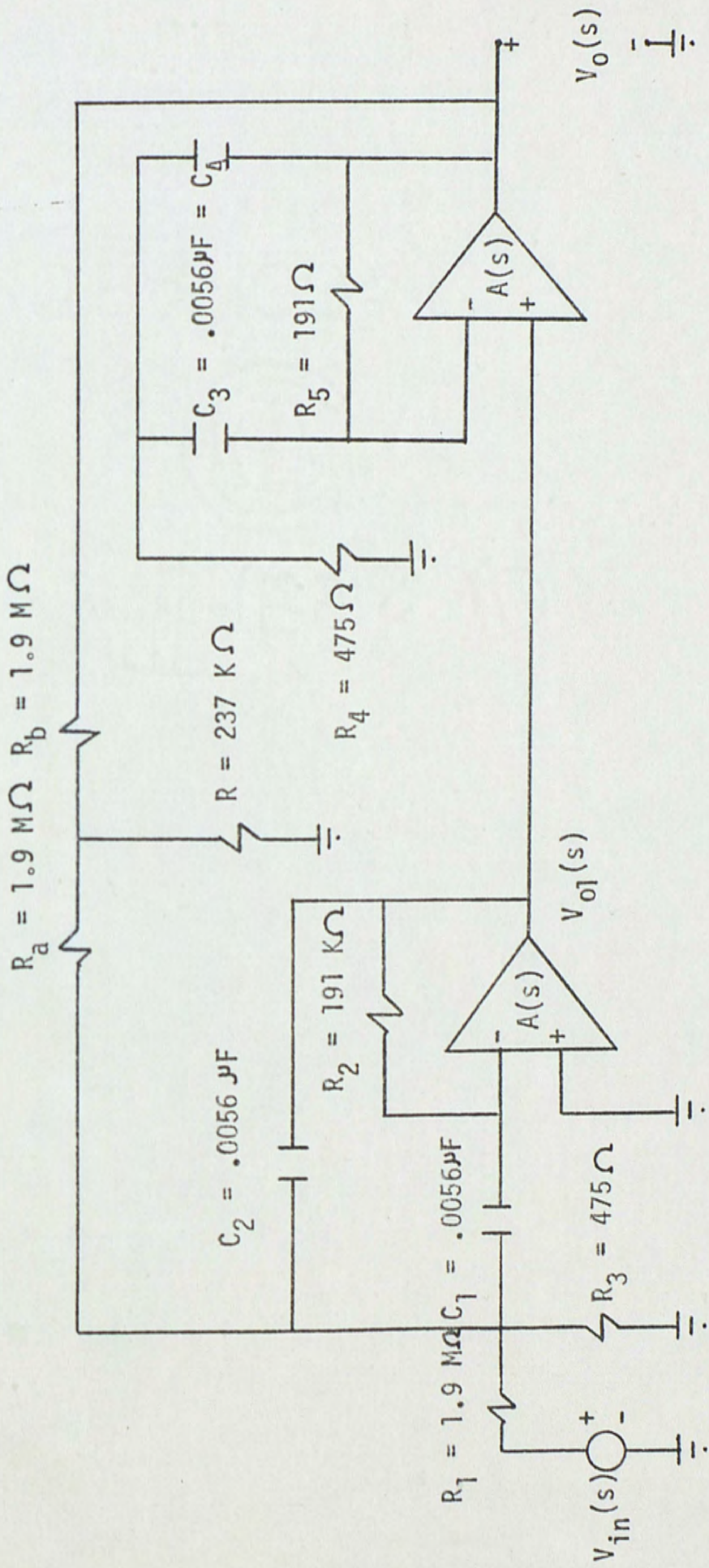Figure 17. The Tee equivalent for R_6

Figure 18. The completed design for the filter under consideration.

Table 1 shows the calculated resistors and capacitors values vs. the experimental resistors and capacitors values.

<div align="center">Table 1</div>

Calculated values	Experimental values	Units
$R_3 = R_4 = 473$	475	ohms
$R_2 = R_5 = 193$	191	Kohms
$R_6 = 19$	19	Mohms
$R_1 = 1.90$	1.90	Mohms
$C_1 = C_2 = C_3 = C_4$		
$= 0.0056$	0.0056	μFarad

The op amp used in Figure 18 is a DUAL TL082M, which has a high input impedance, continuous short circuit protection, wide common mode and differential voltage range, no frequency compensation required, low power consumption, gain and phase match between amplifiers and high slew rate about 7 V/μs.

The gain transfer function of the band-pass filter designed is found as follows:

The first step is to change the frequency scale of equation (77), this is achieved by replacing p in equation (77) by $p/2\pi(424)$. The resulting function $G_{11p}(p)$ is:

$$G_{11p}(p) = \frac{7.097(10^7)}{p^2 + 3.767(10^3)p + 7.097(10^6)} \tag{78}$$

The radian center frequency $w_0 = 2\pi \times 3000$ and the transformation is:

$$p = \frac{s^2 + 3.553(10^8)}{s} \tag{79}$$

Substitution of equation (79) in equation (78) yields the band-pass gain transfer function $G_{bp}(s)$.

$$G_{bp}(s) = \frac{7.097(10^7)s^2}{s^4 + 3.767(10^3)s^3 + 7.17697(10^8)s^2} \cdots$$

$$\cdots \frac{}{+ 1.33841(10^{12})s + 1.26238(10^{17})} \tag{80}$$

Since $G(jw)$ can be considered as $G(s)$ evaluated for $s=jw$, hence for different values of w substituted in equation (80), one can compute the theoretical amplitude response for equation (80). See Table 2.

Table 2 shows the calculated amplitude response values (gain in dB) for equation (80) vs. the experimental values of Figure 18.

Table 2

Frequency KHz	Calculated Gain, dB	Experimental Gain, dB	Percent Error
2.5	3.44	2.9	15.6%
2.7	9.52	10.0	4.8%
2.8	16.68	15.2	8.8%
2.9	18.74	19.3	2.9%
3.1	19.57	19.3	1.4%
3.2	18.16	19.3	6.2%
3.3	14.12	15.0	6.2%
3.4	9.93	10.0	0.7%
3.7	1.02	1.3	27.0%

Figure 19 shows the sketch of gain in dB vs. the frequency in KHz for equation (80). Also Figure 19 shows the sketch of gain in dB vs. the frequency in KHz for Figure 18. Note that in Figure 19,'O' stands for the calculated values and 'x' stands for the experimental values.
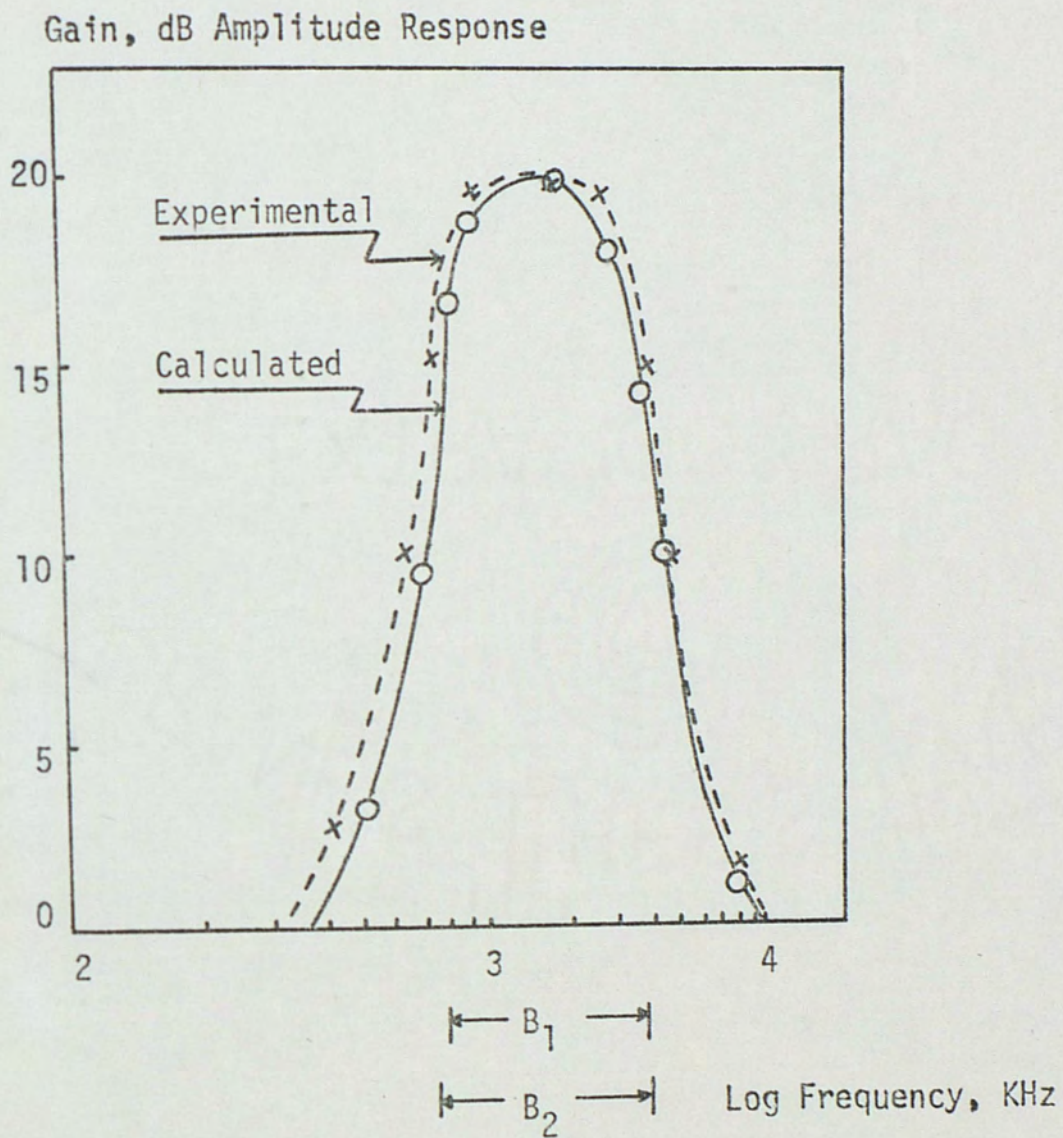
Figure 19. Plot of Gain vs. Frequency for equation (80) and for Figure 18.

CONCLUSION

The purpose of this paper was fulfilled. Two popular
multicoupled filters, the LF and the FLF were discussed, and a
new design method based on Mason's loop rule was developed.
In all three designs the negative feedback topology was used
(Figure 2), that shows low passive sensitivities.

Comparing the three designs, the new design does not use
an extra amplifier for summation nor multicoupling, thus it makes
it economically attractive because it uses fewer parts.

In discussing the results of the design example section, one
can see that there are two amplitude response plots (Gain, dB vs.
Frequency, KHz). The first of the two responses is the theoreti-
cal plot, which is the calculated values of different frequencies
in equation (80). The second of the two responses is the measured
values of the model built (Figure 18) and the values were measured
by means of an oscilloscope. Table 2 shows the tabulated results
of both plots. Table 2 also shows the percent error values at
different points. From the percent error values and Figure 19,
one can see the difference between the calculated results and the
experimental results. The overall percent error is less than seven
percent which is due to: a) Human error in reading the values from
the oscilloscope, b) The percent tolerance of the components which
deviate from their nominal values due to manufacturing tolerances,

45

temperature and humidity changes, and due to chemical changes that occur with the aging of the elements and c) Assuming an ideal op amp.

The bandwidth of the designed example at 3 dB is B = 424 Hz. From Figure 19 B_1 (calculated) is equal to 424 Hz and B_2 (experimental) is equal to 450 Hz. The percent error of B_1 calculated vs. B_2 experimental is:

$$\% \text{ Error of B } = \frac{424 - 450}{424} \text{ X } 100$$

$$= 6.1\%$$

Finally other methods should be investigated to improve the new design method. The primary calculations show that a suggested method to increase the value of the pole Q_0 which is equal to $1/2 \ (R_2/R_1)^{1/2}$ in equation (13) for $C_1 = C_2$ is the use of the positive feedback topology in the negative feedback topology. This improves the value of Q_0 which was limited to the resistance ratio.

BIBLIOGRAPHY

Drayanani, G. _Principle of Active Network Synthesis Design_. New York: John Wiley and Son, 1976.

Dorf, R.C. _Modern Control Systems_. Phillipines: Addison Wesley Publishing Co., 1974.

Gadenz, R.N. "On Low-Sensitivity Realizations of Band-Elimination Active Filters." In _IEEE 1976 Circuits and Systems Symposium_. New York: IEEE, 1976.

Laker, K.R. and Ghausi, M.S. "A Low Sensitivity Multiloop Feedback Active RC Filter." In _IEEE 1973 Circuit Theory_. New York: IEEE, 1973

Martin, R.J. "Multicoupled Band-Pass Filter Design using a Multiple Feedback Configuration." Master thesis. Florida Technological University, Florida, 1976.

Mitra, S.K. _Active Inductorless Filters_. New York: IEEE, 1976.

Stanley, W.D. _Digital Signal Processing_. Reston, Va.: Reston Publishing Co., 1975.

Szentirmai, G. _Computer-Aided Filter Design_. New York: IEEE Press, 1973.

Tow, J. and Kuo, Y.L. "Coupled-Biquad Active Filters." In _IEEE 1972 International Symposium on Circuit Theory_. New York: IEEE, 1972

Zverev, A.I. _Handbook of Filter Synthesis_. New York: John Wiley and Sons, 1976.